Pergamon

Int. J. Solids Structures Vol. 35, Nos 34–35, pp. 5021–5031, 1998

Printed in Great Britain
0020-7683/98/$—see front matter

PII: S0020-7683(98)00107-3

POROHYPERELASTIC–TRANSPORT–SWELLING THEORY, MATERIAL PROPERTIES AND FINITE ELEMENT MODELS FOR LARGE ARTERIES

B. R. SIMON,*† M. V. KAUFMAN,‡ J. LIU† and A. L. BALDWIN§

† Department of Aerospace and Mechanical Engineering Department; The University of Arizona, Tucson, AZ 85721, U.S.A.; ‡ The Hewlett-Packard Company, Palo Alto, CA, U.S.A.; § Department of Physiology, The University of Arizona, Tucson, AZ 85721, U.S.A.

(*Received* 24 *July* 1997; *in revised form* 25 *February* 1998)

Abstract—A porohyperelastic–transport–swelling (PHETS) model is presented in which a soft hydrated tissue material is viewed as a continuum composed of an incompressible porous solid (fibrous matrix) that is saturated by an incompressible fluid (water) in which a mobile species (solute) is dissolved. This PHETS theoretical model is implemented using a finite element model (FEM) including inherent nonlinearity, coupled transport processes, and complicated geometry and boundary conditions associated with soft tissue structures. The PHETS material properties are clearly identified with a physical basis describing and quantifying elasticity, permeability, diffusion, convection, and osmotic properties. The equivalence between the PHETS and the triphasic (TRI) model (Lai *et al.*, 1991) is established using the phenomenological equations, and mathematical expressions are given to relate the PHETS and TRI material properties. A principle of virtual velocities (PVV) links Eulerian and Lagrangian PHETS formulations and provides correspondence rules between the Eulerian and the Lagrangian field variables and material properties. The PVV is also the basis for a mixed Lagrangian PHETS FEM (Kaufmann, 1996), which was developed for the analysis of soft hydrated tissues. Selected PHETS FEM results are presented in order to demonstrate the capability of the PHETS model to simulate coupled deformation, stress, mobile water flux, and albumin flux in the arterial wall undergoing finite straining associated with pressurization, axial stretch, and changes in albumin concentration in bath solutions surrounding a segment of rabbit thoracic aorta. Values for isotropic material parameters and specific details of the experiments and data-reduction methods were obtained from Simon *et al.* (1997; 1998).

INTRODUCTION

Numerous theoretical, experimental, and finite element models (FEMs) have been developed for the study of soft hydrated biological tissues. These models must include material nonlinearity, finite deformation, transport of mobile tissue fluid, and coupled electrical–mechanical–chemical effects associated with mobile charged species. Representative research projects using this modeling view in biomechanics were reviewed by Simon (1992). More recent work includes the papers by Houben (1996), Leventson *et al.* (1997), Simon *et al.* (1996), Snijders *et al.* (1995), and Vankan *et al.* (1997). We also note that the geomechanics and soil mechanics literature provides a large number of references in which such theories are described, e.g., the early work by Biot (1972) extended the poroelastic theory to include large strains and material nonlinearity. During the last decade, a number of soft tissue–transport studies have been based upon the fundamental papers by Lai *et al.* (1991) and Gu *et al.* (1993), which described a triphasic (TRI) theory for the analysis of such soft tissue structures. The TRI model defines soft tissue as a three-phase (or multi-phase) mixture, i.e., the solid phase and the mobile fluid and ionic phase(s). In this paper, we will present a porohyperelastic–transport–swelling (PHETS) model, described by Kaufmann (1996), in which physically based material properties are identified that can be measured experimentally for soft tissues (here rabbit aortas). In this PHETS model, the hydrated tissue is viewed as a continuum composed of an incompressible porous solid (fibrous matrix) that is saturated by an incompressible fluid (water) in which mobile species (solutes) are dissolved. We demonstrate the equivalent of the PHETS and TRI models and

* Author to whom correspondence should be addressed.

give equations that can be used to relate the PHETS material properties to the TRI material properties. The PHETS formulation forms the basis for the development of finite element models (FEMs) that allow the highly nonlinear, coupled PHETS field equations to be solved for complex biological structures.

The objective of this paper is to present a specialized *isotropic* PHETS theory, in both Eulerian and Lagrangian forms, that can be implemented using FEMs of soft hydrated tissues. The isotropic models described here will consider a single neutral species; however, the theory and FEMs can be extended to the anisotropic case for charged species (see Kaufmann, 1996). This extended formulation can be utilized once appropriate experimental data and anisotropic material properties are available. A mixed formulation will be used since both the solid and fluid materials are assumed to be incompressible. The PHETS model will have general applications to various soft tissue structures, but will only be illustrated for mechanical and transport (water and albumin) analysis of *in situ* rabbit thoracic aortas. We begin with the development of the field equations in order to identify necessary material properties and provide the basis for the PHETS FEMs.

POROHYPERELASTIC–TRANSPORT–SWELLING (PHETS) FIELD EQUATIONS

Preliminary definitions and fundamental fields

The displacements and solid velocity at x_i and t are

$$u_i = x_i - X_i = u_i^s = x_i^s - X_i^s, \quad v_i = \dot{u}_i = v_i^s = \dot{u}_i^s = \frac{\mathrm{d}u_i^s}{\mathrm{d}t} \tag{1}$$

where a superposed dot denotes the material time derivative defined with respect to the solid, i.e.,

$$\dot{(\,)} \equiv \frac{\mathrm{d}}{\mathrm{d}t}(\,) \equiv \frac{\partial}{\partial t}(\,)\bigg|_{X_i} = \frac{\partial}{\partial t}(\,)\bigg|_{x_i} + v_k^s \frac{\partial}{\partial x_k}(\,) \tag{2}$$

Superscripts s, f, and c denote the solid, fluid, and species respectively. The apparent relative fluid and the apparent species velocities are

$$v_i^{\mathrm{fr}} = n(v_i^f - v_i^s), \quad v_i^{\mathrm{cr}} = n(v_i^c - v_i^s) \tag{3}$$

where v_i^f is the average velocity of the fluid at x_i and t, defined so that the fluid volume flow rate through a unit area perpendicular to the x_i-axis is nv_i^f. Similarly, v_i^c is the average velocity of the species at x_i and t, defined so that the apparent relative species velocity is arbitrarily defined by eqn (3). The porous solid material in soft tissues is assumed incompressible and is also assumed to be saturated by an incompressible mobile fluid so that the porosity is $n = \mathrm{d}V^f/\mathrm{d}V = 1 - J^{-1}(1 - \mathrm{n}_0)$, with $n_0 = \mathrm{d}V_0^f/\mathrm{d}V_0$. The subscript 0 denotes the reference configuration at X_i and t. The species is considered to be dissolved in the fluid so that species concentration is defined in terms of the fluid volume as

$$c = \frac{\mathrm{d}m^c}{\mathrm{d}V^f} \tag{4}$$

The total volume $\mathrm{d}V = \mathrm{d}V^s + \mathrm{d}V^f$, i.e., the volume of the dissolved mobile species is neglected. Some fundamental measures of deformation include the volume strain, deformation gradient, and Finger's strain, i.e.,

$$J = \frac{dV}{dV_0} = \det F_{ij}, \quad F_{ij} = \frac{\partial x_i}{\partial X_j}, \quad H_{ij} = F^{-1}_{im} F^{-1}_{jm} \tag{5a,b,c}$$

When both solid and fluid materials are incompressible, the true densities $\rho^s_T = dm^s/dV^s$ and $\rho^f_T = dm^f/dV^f$, are constant and a constraint is obtained of the form

$$\frac{\partial v^{fr}_k}{\partial x_k} + \frac{\partial v_k}{\partial x_k} = 0 \tag{6}$$

Cauchy (true) stress measures include the total Cauchy stress, σ_{ij}, the "solid" stress, σ^s_{ij}, and the "pore fluid stress," σ^f_{ij}, which is considered to be hydrostatic so that $\sigma^f_{ij} = \pi^f \delta_{ij}$, with $\pi^f = -$(pore fluid pressure).

Equivalence of PHETS and TRI models

The equivalence of the PHETS and TRI models is based on the phenomenological equations. In the TRI model, these equations relate gradients in mechanical stresses (σ^s_{ij}, π^f) and gradients in chemical potentials (μ^s, μ^f, μ^c) to drag forces associated with differences in *absolute* constituent velocities (see Lai *et al.*, 1991). The isotropic phenomenological equations (see Kaufmann, 1996 for anisotropic forms) are

$$\frac{\partial}{\partial x_j}[(1-n)\sigma^s_{ij}] + \frac{\partial n}{\partial x_i}\pi^f - (1-n)\rho^s_T \frac{\partial \mu^s}{\partial x_i} = f^{sf}(v^s_i - v^f_i) + f^{sc}(v^s_i - v^c_i) \tag{7a}$$

$$\frac{\partial}{\partial x_i}[n\pi^f] - \frac{\partial n}{\partial x_i}\pi^f - n\rho^f_T \frac{\partial \mu^f}{\partial x_i} = f^{fs}(v^f_i - v^s_i) + f^{fc}(v^f_i - v^c_i) \tag{7b}$$

$$-nc\frac{\partial \mu^c}{\partial x_i} = f^{cs}(v^c_i - v^s_i) + f^{cf}(v^c_i - v^f_i) \tag{7c}$$

and form the basis for the TRI model. Introducing total stress, $\sigma_{ij} = (1-n)\sigma^s_{ij} + n\pi^f \delta_{ij}$, and the relative velocities definitions, $v_i = v^s_i$, $v^{fr}_i = n(v^f_i - v^s_i)$, and $v^{cr}_i = n(v^c_i - v^s_i)$, in eqn (7) yields the phenomenological equations expressed in terms of *relative* velocities as

$$\frac{\partial \sigma_{ij}}{\partial x_j} = 0 \tag{8a}$$

$$n^2\left(\frac{\partial \pi^f}{\partial x_i} - \rho^f_T \frac{\partial \mu^f}{\partial x_i}\right) = a^{ff} v^{fr}_i - a^{fc} v^{cr}_i \tag{8b}$$

$$-n^2 c \frac{\partial \mu^c}{\partial x_i} = -a^{cf} v^{fr}_i + a^{cc} v^{cr}_i \tag{8c}$$

Here, eqn (8a) is obtained by replacing eqn (7a) with the sum of eqns (7a–7c). Also note that $(1-n)\rho^s_T(\partial \mu^s/\partial x_i) + n\rho^f_T(\partial \mu^f/\partial x_i) + nc(\partial \mu^c/\partial x_i) = 0$. Now eqns (7) and (8) provide the relations between the TRI and the PHETS phenomenological coefficients, i.e., $a^{ff} = f^{fs} + f^{fc}$, $a^{fc} = a^{cf} = f^{fc} = f^{cf}$, and $a^{cc} = f^{cs} + f^{cf}$, thus relating material properties of the PHETS model to those of the TRI model. Various equivalent formulations are possible, e.g. here we present a mixed PHETS model where u_i, π^f, and c are the primary fields and v^{fr}_i and v^{cr}_i are eliminated from the theory. This is accomplished by solving eqn (8c) for v^{cr}_i as

$$v^{cr}_i = (a^{cc})^{-1}\left(a^{cf} v^{fr}_i - n^2 c \frac{\partial \mu^c}{\partial x_i}\right) \tag{9}$$

and substituting eqn (9) into eqn (8b) to obtain the Darcy law (eqn 12b, below) and

substituting eqn (9) into the definition for relative species flux, $f_i^{cr} \equiv cv_i^{cr}$, to obtain eqn (12c, below).

Mixed Eulerian PHETS model

The field equations now include (a) the conservation equations (total momentum, mass of solid and fluid, and mass of the species)

$$\frac{\partial \sigma_{ji}}{\partial x_j} = 0, \quad \frac{\partial v_j^{fr}}{\partial x_j} + D_{kk} = 0, \quad \frac{\partial}{\partial t}(nc) + \frac{\partial f_i^{cr}}{\partial x_i} + \frac{\partial}{\partial x_i}(ncv_i) = 0 \tag{10a,b,c}$$

(b) the kinematic equations (Eulerian strain, velocity strain, pore fluid pressure gradient, and concentration gradient)

$$E_{ij}^{*} = \tfrac{1}{2}(\delta_{ij} - F_{ki}^{-1}F_{kj}^{-1}), \quad D_{ij} = \tfrac{1}{2}\left(\frac{\partial v_i}{\partial x_j} + \frac{\partial v_j}{\partial x_i}\right), \quad e_i^{\pi} = \frac{\partial \pi^{f}}{\partial x_i}, \quad e_i^{c} = \frac{\partial c^{c}}{\partial x_i} \tag{11a,b,c,d}$$

and (c) the constitutive equations ("effective stress," σ_{ij}^{e}, generalized Darcy law, and relative species flux)

$$\sigma_{ij} = \sigma_{ij}^{e} + \pi^{f}\delta_{ij}, \quad v_i^{fr} = k^{ff}\left(e_i^{\pi} + \frac{\partial \pi^{c}}{\partial x_i}\right), \quad f_i^{cr} = -d^{cc}e_i^{c} + b^{cf}cv_i^{fr} \tag{12a,b,c}$$

Equations (10–12) are the isotropic form of the PHETS initial boundary value problem. We have assumed no strain dependence in the chemical potentials μ^{f} and μ^{c} (see Kaufmann, 1996 for a more general anisotropic formulation including this strain dependence). The necessary PHETS material properties are the effective stress, σ_{ij}^{e}, the hydraulic permeability, k^{ff}, the osmotic pressure gradient, $\partial \pi^{c}/\partial x_i$, and the diffusion and convection coefficients, d^{cc} and b^{cf}. One can relate the set of PHETS material properties to the set of TRI properties using these definitions and the relations between the phenomenological coefficients above, thereby allowing either set of properties to be used in the analysis process.

Principles of virtual velocities

The Eulerian and Lagrangian principles of virtual velocities (PVV) form a basis for FEMs, as well as identifying the appropriate correspondence rules for stresses and relative velocities in the formulation of the PHETS field problem. The Eulerian PVV in mixed form is

$$\int_V \delta D_{ij}\sigma_{ji}^{e}\,dV + \int_V \delta D_{kk}\pi^{f}\,dV - \int_A \delta v_i \sigma_{ij}\hat{n}_j\,dA = 0 \tag{13a}$$

$$\int_V \delta\pi^{f} D_{kk}\,dV - \int_V \delta e_i^{\pi}k^{ff}e_i^{\pi}\,dV - \int_V \delta e_i^{\pi}k^{ff}\frac{\partial \pi^{c}}{\partial x_i}dV + \int_A \delta\pi^{f}v_k^{fr}\hat{n}_k\,dA = 0 \tag{13b}$$

$$\int_V \delta\dot{c}\frac{\partial}{\partial t}(nc)\,dV - \int_V \delta\dot{e}_i^{c}f_i^{cr}\,dV + \int_V \delta\dot{c}\frac{\partial}{\partial x_i}(ncv_i)\,dV + \int_A \delta\dot{c}f_i^{cr}\hat{n}_i\,dA = 0 \tag{13c}$$

where $\hat{n}_i$ is the unit normal to the area dA. Using appropriate correspondence rules, eqn (13) can be transformed into a mixed Lagrangian PVV of the form

$$\int_{V_0} \delta \dot{E}_{ij} S^{e}_{ji} \, dV_0 + \int_{V_0} \delta \dot{E}_{ij} H_{ij} \pi^{f} J \, dV_0 - \int_{A_0} \delta \dot{u}_i T_{ji} \hat{n}_{0j} \, dA_0 = 0 \tag{14a}$$

$$\int_{V_0} \delta \pi^{f} \dot{E}_{ij} H_{ij} J \, dV_0 - \int_{V_0} \delta \tilde{e}^{\pi}_i \tilde{k}_{ij} \tilde{e}^{\pi}_j \, dV_0 - \int_{V_0} \delta \tilde{e}^{\pi}_i \tilde{k}_{ij} \frac{\partial \pi^{c}}{\partial X_j} dV_0 + \int_{A_0} \delta \pi^{f} \tilde{v}^{fr}_k \hat{n}_{0k} \, dA_0 = 0 \tag{14b}$$

$$\int_{V_0} \delta \dot{c} \frac{d}{dt}(Jnc) \, dV_0 - \int_{V_0} \delta \tilde{e}^{c}_i \tilde{j}^{cr}_i \, dV_0 + \int_{A_0} \delta \dot{c} \tilde{j}^{cr}_i \hat{n}_{0i} \, dA_0 = 0 \tag{14c}$$

where $\hat{n}_{0i}$ is the unit normal to the area dA_0. In the total Lagrangian formulation, all field variables are considered to be dependent on X_i and t, i.e., the displacement is $u_i = u_i(X_j, t) = x_i - X_i$, $\pi^{f} = \pi^{f}(X_j, t)$, $c = c(X_j, t)$, etc. The relations between field variables described in the Eulerian and Lagrangian PVV allow the identification of correspondence rules. The classical correspondence rules relate Cauchy stress to the first and second Piola–Kirchhoff stresses (defined below). The relative fluid velocity and relative species velocity are also related by correspondence rules. Then v^{fr}_i can be referred, in the Lagrangian sense, to the reference configuration by defining a Lagrangian relative fluid velocity, $\tilde{v}^{fr}_i$, that corresponds to v^{fr}_i so that the same relative fluid mass flow rate occurs through areas dA and dA_0, i.e., $\rho^{f}_T v^{fr}_i \hat{n}_i \, dA = \rho^{f}_{T0} \tilde{v}^{fr}_i \hat{n}_{0i} \, dA$. A similar correspondence rule applies to relative species velocities, $\tilde{v}^{cr}_i$ and v^{cr}_j; i.e., with definitions of Eulerian and Lagrangian relative species flux given as $j^{cr}_i = c v^{cr}_i$ and $\tilde{j}^{cr}_i = c \tilde{v}^{cr}_i$, the correspondence is $j^{cr}_i \hat{n}_i \, dA = \tilde{j}^{cr}_i \hat{n}_{0i} \, dA_0$ (equal relative species flux through corresponding areas dA and dA_0). Then, for an incompressible fluid ($\rho^{f}_T = \rho^{f}_{T0}$) with $c(x_i, t) = c(X_i, t)$ and using the Nanson formula, $\tilde{v}^{fr}_i$ corresponds to v^{fr}_i and $\tilde{v}^{cr}_i$ to v^{cr}_i as $\tilde{v}^{fr}_i = J(\partial X_i / \partial x_j) v^{fr}_j$ and $\tilde{v}^{cr}_i = J(\partial X_i / \partial x_j) v^{cr}_j$.

Mixed Lagrangian PHETS model

The mixed Lagrangian field equations are (a) the conservation equations (total momentum, mass of solid and fluid, and species mass),

$$\frac{\partial T_{ji}}{\partial X_j} = 0, \quad \frac{\partial \tilde{v}^{fr}_j}{\partial X_j} + J H_{ij} \dot{E}_{ij} = 0, \quad \frac{d}{dt}(nJc) + \frac{\partial \tilde{j}^{cr}_i}{\partial X_i} = 0 \tag{15a,b,c}$$

where the first and second Piola–Kirchhoff stresses are $T_{ij} = J F^{-1}_{jk} \sigma_{ki}$ and $S_{ij} = J F^{-1}_{im} \sigma_{mn} F^{-1}_{jn}$, respectively; (b) the kinematic equations (Green's strain, pore fluid pressure gradient, and concentration gradient)

$$E_{ij} = \tfrac{1}{2}(F_{ki} F_{kj} - \delta_{ij}), \quad \tilde{e}^{\pi}_i = \frac{\partial \pi^{f}}{\partial X_i}, \quad \tilde{e}^{c}_i = \frac{\partial c}{\partial X_i} \tag{16a,b,c}$$

and (c) the constitutive equations (effective total second Piola–Kirchhoff stress, S^{e}_{ij}, generalized Darcy law, and the relative species flux)

$$S_{ij} = S^{e}_{ij} + J \pi^{f} H_{ij}, \quad \tilde{v}^{fr}_i = \tilde{k}_{ij} \left(\tilde{e}^{\pi}_j + \frac{\partial \pi^{c}}{\partial X_j} \right), \quad \tilde{j}^{cr}_i = -\tilde{d}^{cc}_{ij} \tilde{e}^{c}_j + \tilde{b}^{cf} c \tilde{v}^{fr}_i \tag{17a,b,c}$$

We now have corresponding Eulerian and Lagrangian PHETS theories that provide partial differential equations to be solved for u_i, π^{f}, and c subject to boundary conditions and initial conditions.

ISOTROPIC PHETS MATERIAL PROPERTIES

We consider a single, neutral species (with no strain dependence in μ^{f} and μ^{c}) using corresponding sets of Eulerian and Lagrangian material properties for the PHETS model(s). The Eulerian material properties are: (a) solid—generalized hyperelastic drained strain

energy density function U^e, defining the effective stress as $\sigma^e_{ij} = J^{-1}F_{im}(\partial U^e/\partial E_{mn})F_{nj}$; (b) fluid—hydraulic permeability, $k^{ff} = n^2[a^{ff} - a^{fc}(a^{cc})^{-1}a^{cf}]^{-1}$ and osmotic pressure gradient, $\partial\pi^c/\partial x_i = g^c e^c_i$, with osmotic coefficient, $g^c = -[a^{fc}(a^{cc})^{-1}c(\partial\mu^c/\partial c) + \rho^r_T(\partial\mu^f/\partial c)]$; and (c) species—diffusion and convection coefficients, $d^{cc} = n^2 c(\partial\mu^c/\partial c)$ and $b^{cf} = (a^{cc})^{-1}a^{cf}$. In addition, the porosity, n_0, is needed in $n = 1 - J^{-1}(1 - n_0)$. The PVV provides the correspondence rules relating Eulerian fields to the Lagrangian fields, thus determining mathematical relations between the Eulerian and Lagrangian material property functions. Note that although the Eulerian forms are isotropic, the corresponding Lagrangian forms are not isotropic. The Lagrangian properties include: (a) solid—generalized hyperelastic effective strain energy density function, U^e, defining $S^e_{ij} = \partial U^e/\partial E_{ij}$; (b) fluid—hydraulic permeability, $\tilde{k}^{ff}_{ij} = Jk^{ff}H_{ij}$, and osmotic coefficient, $\tilde{g}^c = g^c$; and (c) species—diffusion coefficient, $\tilde{d}^{cc}_{ij} = Jd^{cc}H_{ij}$, and convection coefficient, $\tilde{b}^{cf} = b^{cf}$. For isotropic materials, by the principle of equipresence, all material property functions are dependent on the strain invariants $\bar{I}_1$, $\bar{I}_2$, J, and c; e.g., $U^e = U^e(\bar{I}_1, \bar{I}_2, J, c)$, $\tilde{k}^{ff}_{ij} = \tilde{k}^{ff}_{ij}(\bar{I}_1, \bar{I}_2, J, c)$, etc., where $\bar{I}_1 = J^{-2/3}I_1$ and $\bar{I}_2 = J^{-4/3}I_2$ are deviatoric strain invariants with $I_1 = 3 + 2E_{kk}$ and $I_2 = 3 + 4E_{kk} + 2[E_{ii}E_{jj} - E_{ij}E_{ij}]$. Specific forms for these material properties and material parameters will be given for rabbit aortic tissues based on experimental observations.

FINITE ELEMENT MODEL (FEM)

There are several possible formulations for finite element models, e.g., Eulerian porohyperelastic FEMs in ABAQUS, Lagrangian porohyperelastic (mixed, penalty, etc.) FEMs, Lagrangian biphasic (mixed, penalty, etc.) FEMs, mixed TRI FEMs, etc. Note that the ABAQUS can be used for porohyperelastic or biphasic models, but cannot be used directly for the development of PHETS or TRI FEMs where species transport is included. We have developed a mixed, total Lagrangian PHETS FEM program for the analysis of coupled structural-transport processes in soft hydrated tissues. Using the (bold-faced) matrix notation $\boldsymbol{u} = \{u_i\}$, etc., this mixed Lagrangian FEM is based on interpolations in each finite element of the form $\boldsymbol{u} = \mathbf{N}_u\bar{\boldsymbol{u}}$ (quadratic) and $\pi^f = \mathbf{N}_\pi\bar{\pi}$ and $c = \mathbf{N}_c\bar{\mathbf{c}}$ (both linear) to form the quasi-static assembled global system of equations for the FEM

$$\mathbf{C}\dot{\mathbf{r}} + \mathbf{R}^{int} = \mathbf{R}^{ext} \tag{18}$$

Then the boundary and initial conditions are prescribed, and a time integrator is applied (e.g., a backward difference with Newton–Rapheson iteration) to determine $\mathbf{r}(t)$, which contains elemental $\bar{\mathbf{u}}$, $\bar{\pi}$, and $\bar{\mathbf{c}}$. A modified Petrov–Galerkin method (Yu and Heinrich 1986, 1987) was introduced to provide accurate solutions for the situations where there is significant convective flux (and relatively large Peclet numbers) in the arterial wall tissues. The PHETS FEM program was verified using analytical solutions and simulations of rubber tubes and arteries. The transport analysis capability of the program was verified by comparison of FEM and analytical solutions for diffusion-convection problems. We will not present the details of the finite element formulation and program here and refer the reader to Kaufmann (1996) for further specific information.

A FEM was developed to represent a segment of rabbit aorta as a layered cylinder (intima and media) in a state of axisymmetric, plane strain (see Fig. 1). The FEM was

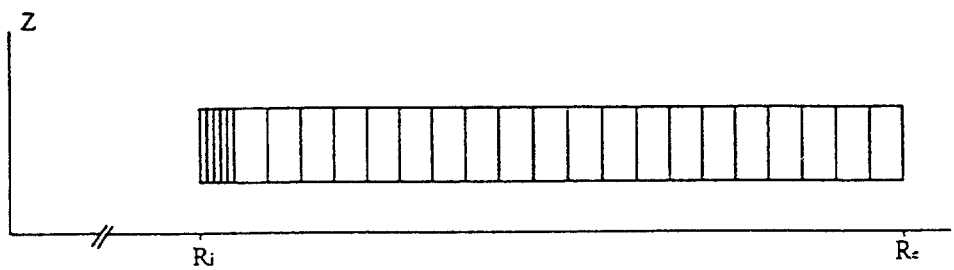

Fig. 1. Axisymmetric plane strain PHETS FEM of a rabbit aorta including intima (*I*) and media (*M*). The adventitia was removed in the experiments.

subjected to initial and boundary conditions representing internal pressure, axial stretch, and prescribed species concentration in the bath solutions at the internal and/or external surfaces of the models. The FEM (converged mesh) was composed of 43 elements (4 thin elements for the intima and 39 elements for the media). The adventitia was removed in the experiments and was not included in these FEMs. These FEMs were also used as the basis for the data-reduction procedures, which provided the necessary material parameters. Representative FEM results are given here for rabbit aortic sections undergoing finite strain and subjected to mechanical forces and pressures as well as concentration gradients in albumin (considered as a single neutral species dissolved in the fluid).

PHETS MATERIAL PROPERTIES FOR RABBIT AORTAS

The experimental data were obtained from rabbit aortas subjected to axial stretch, inflation, and immersion in bath(s) of labeled albumin dissolved in physiological buffered saline (PBS) solution. Data were obtained from our laboratory and from the work of Tedgui and Lever (1985). Mobile water motion in the arterial tissue was determined from the velocity, v_B, of an air bubble introduced in the inflation cannulation tube. Values for v_B were measured at various pressure levels in order to determine aortic (intimal and medial) tissue permeability. The experimental protocols and apparatus are described by Simon *et al.* (1998) and Baldwin *et al.* (1992), and the data-reduction methods by Simon *et al.* (1997). These methods are based on a generalized least-squares approach in which an error,

$$e = \sum_{M=1}^{N_{\text{data}}} (f_M^{\text{model}} - f_M^{\text{exp}})^2, \tag{19}$$

is minimized to determine material parameters. In this expression, $f^{\text{model}} = f^{\text{model}}$ (material parameters) and f^{exp} is the corresponding experimental value, where f^{model} is obtained from either analytical models or from the PHETS FEM. Following are the PHETS material properties and corresponding material parameters that were determined for rabbit aortas: (a) A generalized Fung form for $U^e = (1/2)C_0(e^{\phi} - 1)$, with $\phi = C_1'(\bar{I}_1 - 3) + C_2'(\bar{I}_2 - 3) + K'(J-1)^2$, was quantified using rapid (undrained) inflation to provide values for C_0, C_1', and C_2' and steady-state (drained) inflation ($\pi^f = 0$) to determine K'. (b) Permeabilities ($k_{rr}^{ff} = k$) for the intima and media, k_{INT} and k_{MED} (adventitia removed). Medial and intimal permeabilities were determined using steady-state inflations of de-endothelialized and intact vessels to provide v_B versus P data to minimize e, in which a constant k_{MED} and a nonlinear form for $k_{\text{INT}} = k_{\text{INT}}(P, \lambda)$ were assumed. At the outset, the osmotic pressure term, $\partial\pi^c/\partial r$, was not included in this series of models, but is being introduced in the next phase of this modeling effort. Comparison of FEM and experimental data for $P - \mathbf{r}$ and $v_B - P$ are shown in Figs 2 and 3. (c) Diffusion and convection parameters ($d_{rr}^{cc} = d$, $b_{rr}^{cf} = b$) were quantified as constant. The intimal and medial diffusion coefficients, d_{INT} and d_{MED} (adventitia removed), were determined using rabbit aortas for which $P = 0$ (no convection) and data for labeled albumin concentration profile(s) after 25 min of immersion in internal and external albumin PBS solutions with concentration c_B. The data-reduction program determined values for d_{INT} and d_{MED} to minimize e. Figure 4 illustrates the close agreement between our experimental data and the PHETS FEM using optimal values for d_{INT} and d_{MED} to calculate the albumin concentration profile.

The labeled albumin concentration profiles reported by Tedgui and Lever (1985) were used in our data-reduction procedure to determine intimal and medial b^{cf}, i.e., b_{INT} and b_{MED} (both assumed constant). Tedgui and Lever's experiments (including both diffusion and convection) determined steady albumin concentration profiles for pressurized rabbit aortas for damaged (de-endothelialized) and intact vessels immersed in an external albumin solution with concentration c_B. The data-reduction procedure determined the constants b_{INT} and b_{MED} (using known d_{INT}, d_{MED}, k_{INT}, and k_{MED}) with $P = 70$ and 180 mm Hg for damaged and intact vessels. Figure 5 shows a comparison of results from PHETS and FEMs using these material parameters with data from Tedgui and Lever's experiments.

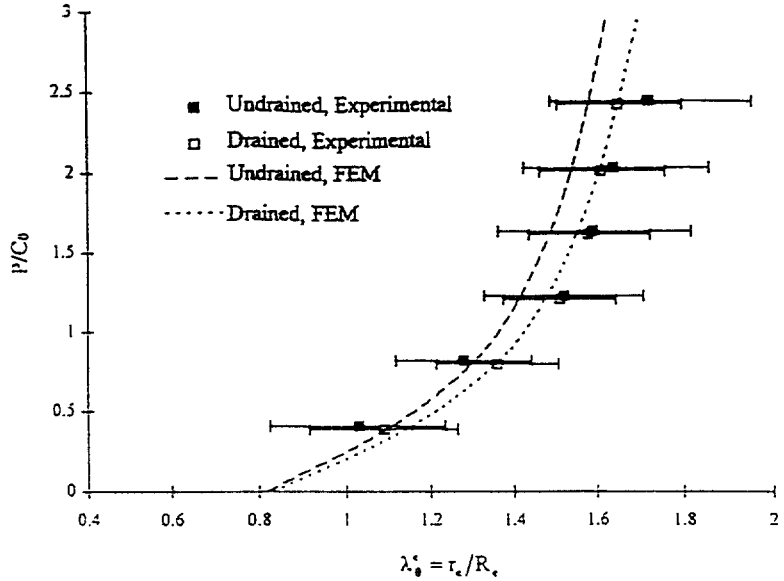

Fig. 2. Experimental and FEM results for internal pressure (P/C_0) vs external radius ($\lambda_\theta^s = r_e/R_e$) data for intact rabbit aortas subjected to undrained (rapid inflation) and drained (steady state inflation, $\pi^f = 0$) conditions.

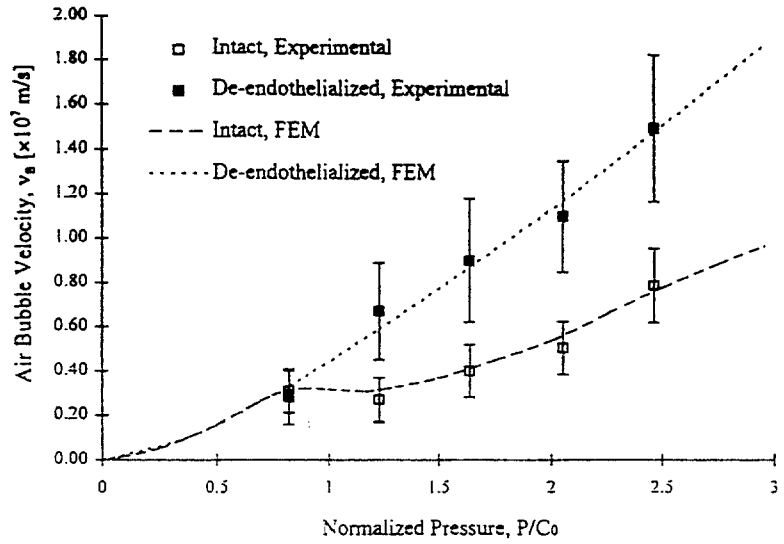

Fig. 3. Experimental and FEM results for air bubble velocity (v_B) vs pressure (P/C_0) data for intact and de-endothelialized rabbit aortas subjected to steady-state pressurization.

The large strains associated with pressurization of the aortas are clearly visible in this figure. Also, the Peclet numbers predicted by the PHETS FEM agreed well with the experimental results. Thus all the required material parameters for this PHETS model were determined for rabbit aortas, i.e., the constants C_0, C_1', C_2', K', k_{MED}, d_{MED}, and b_{MED} for the media and d_{INT} and b_{INT} for the intima, as well as any parameters in the nonlinear form for $k_{INT}(P, \lambda)$. We must emphasize, however, that the intima is a thin, complex layer that is not a PHETS material, but was represented here by finite elements, so that k_{INT}, d_{INT}, and b_{INT} are to be considered as average values (resistance) associated with a thin-layer approximation. Table 1 lists the numerical values for the PHETS material parameters determined for the representative rabbit aortas considered in this paper.

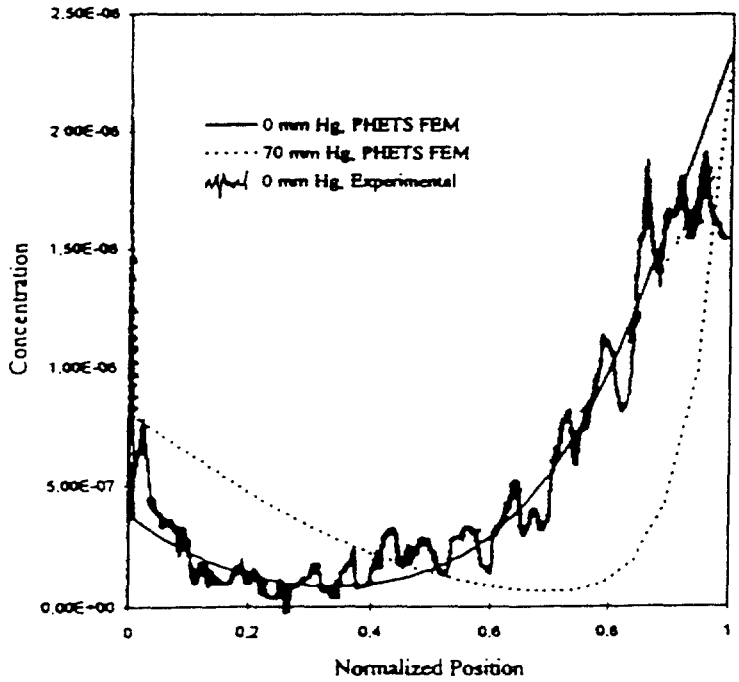

Fig. 4. Labeled albumin concentration in the aortic wall 25 min after immersion in solution of labeled albumin. PHETS FEM results compared to pure diffusion experimental data ($P = 0$) and PHETS FEM results only for diffusion and convection ($P = 70$ mm Hg).

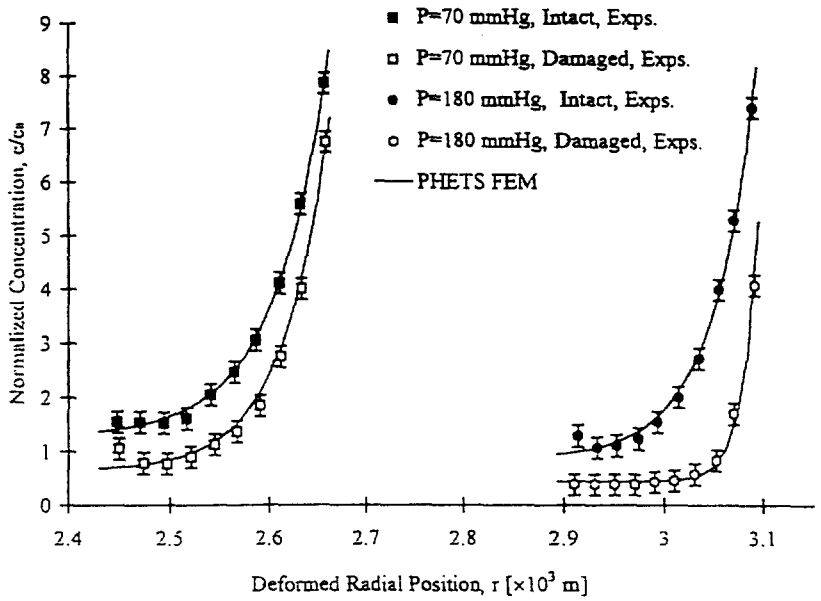

Fig. 5. Steady-state labeled albumin concentration profiles (c/c_B) in the deformed arterial wall: finite element results compared with Tedgui and Lever's (1985) experimental data; c_B = bath concentration of albumin.

An additional simulation was carried out using the PHETS FEM of the rabbit aorta. The FEM of the pure diffusion experiment was subjected to internal fluid pressure, $P = 70$ mm Hg, in order to introduce convection effects in the transport processes in the aortic wall. In this FEM, diffusion occurs from both the internal and external surfaces due to the presence of labeled albumin at these surfaces. In addition, convection of the albumin occurs as relative fluid flux develops due to the mechanical pressure gradient across the aortic wall.

Table 1. Axisymmetric, plane strain, isotropic PHETS material properties

Property	Media (MED)	Intima (INT)
U^e	$U^e_{MED} = 1/2C_0(e^{\phi}-1)$ $\phi = C'_1(\bar{I}_1-3)-C'_2(\bar{I}_2-3)+K'(J-1)^2$ $C_0 = 8130$ N/m^2, $C_1 = 0.907$, $C'_2 = 0.00248$, $K' = 12.5$	U^e_{INT} negligible
$k^{ff}_{ij} \rightarrow k^{ff}_{rr} = k$	$k_{MED} = 1.05 \times 10^{-5}$ m^4/N-s	$k_{INT}(P, \lambda)$ = nonlinear function (Simon *et al*, 1997)
$d^{cc}_{ij} \rightarrow d^{cc}_{rr} = d$	$d_{MED} = 2.93 \times 10^{-13}$ m^2/s	$d_{INT} = 2.69 \times 10^{-15}$ m^2/s
$b^{cf}_{ij} \rightarrow b^{cf}_{rr} = b$	$b_{MED} = 0.150$	$b_{INT} = 0.050$
$(\partial\pi^c/\partial x_i) \rightarrow (\partial\pi^c/\partial r)$	$(\partial\pi^c/\partial r) = g^c_{MED}(\partial c/\partial r)$ not considered	$(\partial\pi^c/\partial r) = g^c_{INT}(\partial c/\partial r)$ not considered

Figure 4 (dashed line) clearly shows the effect of convection in the transport of labeled albumin, i.e., the 25-min albumin concentration profile is "shifted" to the right from the pure diffusion response due to convective transport. The value for b_{INT} reported here corresponds to the diffusion/convection case ($P = 70$ mm Hg) shown in Fig. 4. Additional tests and data reduction will be necessary to determine b_{INT} (and d_{INT}) for the thin intimal layer.

CONCLUSION

This paper has presented a specialized isotropic formulation for the PHETS theory and a mixed PHETS FEM that were used to analyze coupled transport processes of a (neutral) species in the wall of a rabbit aorta. The model can be extended to include anisotropy and multiple charged species (see Kaufmann, 1996). Phenomenological equations provide the basis for the TRI and PHETS models. The phenomenological equations were converted to a PHETS model formulation (either Eulerian or Lagrangian) so that FEMs could be developed and PHETS material properties identified that have physical significance as hyperelasticity and permeability and as osmotic, diffusion, and convection coefficients. These properties were also quantified using specific experiments and data-reduction methods based on systematic procedures (described in related publications) to determine the material parameters in the PHETS material properties (U^e, k_{INT}, k_{MED}, d_{INT}, d_{MED}, b_{INT}, and b_{MED}). We have demonstrated the equivalence of the PHETS model and the TRI model based on the formulation of the phenomenological equations and have given mathematical expressions that can be used to relate material properties in these two models. This means that either PHETS or TRI material properties could be introduced in the PHETS FEMs of a soft hydrated tissue where water and species transport are of interest.

There are a number of directions for future research using the PHETS theory and FEMs. Our isotropic models will lead to anisotropic models once appropriate experimental data are available. The effects of active smooth muscle and pre-stress conditions associated with tissue remodeling (opening angle) can be introduced. We will conduct a more detailed analysis of the complex behavior of the intima (barrier transport function, etc.) at the microscopic level and plan to consider the adventitia in our future arterial models. We are currently considering PHETS models including multiple charged species and $\partial\pi^c/\partial x_i$ in the theoretical and FEM development.

We anticipate specific applications of the PHETS theory and FEMs in the following areas:

(1) fundamental study of artherogenesis at specific initiation sites (branches, etc.) in the walls of arteries;

(2) combine PHETS FEMs with computational fluid dynamic models of the arterial system to consider flows and coupled fluid/structural/transport interactions with flexible vessel walls, again addressing the etiology of atherosclerosis;
(3) develop PHETS FEMs of local drug delivery systems, i.e., simulate the balloon catheter system and local transport processes in the arterial wall;
(4) utilize PHETS theory to model and design "tissue-engineered" arterial grafts (currently being studied in our laboratory) to begin quantifying the processes of tissue in-growth and endothelialization, as well as to help identify mechanical/transport graft responses that may serve as initiators of hyperplasia.

Acknowledgements—The authors gratefully acknowledge support from the National Science Foundation, NSF Grant BES-9410571.

REFERENCES

Baldwin, A. B., Wilson, L. M. and Simon, B. R. (1992) Effect of pressure on aortic hydraulic conductance. *Arteriosclerosis and Thrombosis* **12,** 163–171.
Biot, M. A. (1972) Theory of finite deformations of porous solids. *Indiana Univ. Math. J.* **21,** 597–620.
Gu, W., Lai, W. M. and Mow, V. C. (1993) A generalized triphasic theory for multi-electrolyte transport in charged, hydrated soft tissues. In *Advances in Bioengineering*, ed. M. Askew, ASME BED, Vol. 28, 217–218.
Houben, G. B. (1996) Swelling and compression of intervertebral disc tissue—model and experiment. Ph.D. Thesis, Maastricht University, The Netherlands.
Kaufmann, M. V. (1996) Porohyperelastic analysis of large arteries including species transport swelling effects. Ph.D. Thesis, Aerospace and Mechanical Engineering, The University of Arizona, Tucson.
Lai, M., Hou, J. S. and Mow, V. C. (1991) A triphasic theory for the swelling and deformation behaviors of articular cartilage. *J. Biomech. Engr.* **113,** 245–258.
Leventson, M. E., Frank, E. H. and Grodzinsky, A. J. (1997) Electrokinetic and poroelastic coupling during finite deformations of charged porous media. *J. of Appl. Mech.* (in review).
Simon, B. R. (1992) Multiphase poroelastic finite element models for soft tissue structures. *Appl. Mech. Rev.* **56,** 191–218.
Simon, B. R., Kaufmann, M. V., McAfee, M. A., Baldwin, A. L. and Wilson, L. M. (1998) Identification and determination of material properties for porohyperelastic analysis of large arteries. *J. Biomech. Eng.* **120,** 188–194.
Simon, B. R., Liable, J. P., Pflaster, D S., Yuan, Y.and Krag, M. H. (1996) A poroelastic finite element model formulation including swelling in soft tissue structures. *J. Biomech. Eng.* **118,** 1–9.
Simon, B. R., Liu, J., Kaufmann, M. V. and Baldwin, A. L. (1997) Data reduction methods for determination of material properties for porohyperelastic–transport–swelling (PHETS) finite element of large arteries. *Proceedings of* 1997 *Bioengineering Conference*, ed. K. B. Chandran, R. Vanderby and M. S. Hefzy, ASME BED, Vol. 35, 35–36.
Snijders, H., Huyghe, J. M. and Janssen, J. D. (1995) Triphasic finite element model for swelling porous media. *Int. J. Num. Meth. Fluids* **20,** 1039–1046.
Tedgui, A. and Lever, M. J. (1985) The interaction of convection and diffusion in the transport of ^{131}I-albumin within the media of the rabbit thoracic aorta. *Circ. Res.* **57,** 856–863.
Vankan, W. J., Huyghe, J. M., Drost, M. R., Janssen, J. D. and Huson, A. (1997) A finite element mixture model for hierarchical porous media, 1997. *Int. J. Num. Meth. Eng.* **40,** 193–210.
Yu, C. C. and Heinrich, J. C. (1986) Petrov–Galerkin methods for the time-dependent convective transport equation. *Int. J. Num. Meth. Eng.* **23,** 883–901.
Yu, C. C. and Heinrich, J. C. (1987) Petrov–Galerkin methods for multidimensional time-dependent convective-diffusion equations. *Int. J. Num. Meth. Eng.* **24,** 2201–2215.